LETTERS

1064 nm photoresponse enhancement of femtosecond-laser-irradiated Si photodiodes by etching treatment

Applied Physics Express **11**, 062203 (2018)
https://doi.org/**10.7567/APEX.11.062203**

1064 nm photoresponse enhancement of femtosecond-laser-irradiated Si photodiodes by etching treatment

Ke Wang[1,2], Haigui Yang[1], Xiaoyi Wang[1]*, Yanchao Wang[1]*, Zizheng Li[1], Jinbo Gao[1,2], Borui Li[1,2], and Jinsong Gao[1,2]

[1]*Key Laboratory of Optical System Advanced Manufacturing Technology, Changchun Institute of Optics, Fine Mechanics and Physics, Chinese Academy of Sciences, Changchun 130033, China*
[2]*University of the Chinese Academy of Sciences, Beijing 100039, China*

*E-mail: wangxiaoyi1977@sina.com; spirit0127@126.com

Received April 8, 2018; accepted May 11, 2018; published online May 30, 2018

We propose an etching treatment to improve the photoresponse of a femtosecond (fs)-laser-irradiated silicon photodiode working at 1064 nm. We investigated its surface structure and optical and electrical properties after fs laser irradiation, and further demonstrated the evolution of textured surface morphology, hyperdoping concentration, and crystallinity with etching time. We found that the etching treatment can peel off the hyperdoped layer by an appropriate amount, control the dopant concentration, and repair the crystallinity and subsurface damage of the hyperdoped microstructured silicon induced by fs laser irradiation. Experimental results indicate that the photoresponse at 1064 nm can be enhanced from 0.2 to 0.45 A/W after etching treatment.

To achieve the infrared photoresponse of silicon (Si)-based photodiodes working at 1064 nm, painstaking efforts have been made, because, at present, as the second most abundant element in Earth's crust, Si is a common material for photodiodes, and 1064 nm photodiodes are widely used, such as in laser communications, laser tracking systems, and laser guidance. Unfortunately, 1064 nm light falls on the edge of the Si band gap and its absorption coefficient is as low as 10 cm^{-1},[1)] which limits the 1064 nm response. To enhance its response, a thick Si wafer is generally used for the fabrication of most Si photodiodes. This improvement, however, brings many disadvantages to devices, such as a low response speed and a large resistance, which can inhibit device performance. For full depletion, this kind of detector needs to operate under a high voltage. Additionally, the dark current will be magnified when a high voltage is applied to the detector.

To realize a high-speed and high-sensitivity Si photodiode working at 1064 nm, high absorption near the edge of the Si band gap is strongly required in a thin wafer. As a fascinating approach, femtosecond (fs) laser irradiation has received extensive attention in the absorption enhancement of Si wafers.[2–6)] Under ultrafast laser ablation, an array of micrometer-sized conical spikes with quasi-periodic distribution, which serve as light-trapping structures, which is also referred to as laser-induced periodic surface structures (LIPSSs), can be formed on a Si surface.[7,8)] Moreover, chalcogen elements can be doped on Si, resulting in a hyperdoped layer covered with conical spikes. In this case, electron–electron interaction couples the energy levels into the so-called impurity or intermediate band.[9,10)] It can not only improve the absorption near the edge of the Si band gap effectively, but also extend the absorption limitation to a large wavelength. However, on the one hand, an excessively high chalcogen concentration and a very thick hyperdoped layer can both reduce carrier mobility[11)] and adversely affect carrier transport.[12)] On the other hand, the laser-induced amorphous Si (a-Si),[13–16)] defects[17)] and high-pressure Si phases[18–20)] on the textured surface lead to a decrease in carrier lifetime[21)] and an increase in the dark current of the device. More importantly, the light trapped in the high-density defects produced in the surface layer of microstructured Si cannot be effectively converted into photocurrents.

In this study, we propose an etching treatment to improve the photoresponse of fs-laser-irradiated Si photodiodes working at 1064 nm. First, we investigated the surface structure and optical and electrical properties of Si photodiodes by fs laser irradiation. Then, we demonstrated the evolution of textured surface morphology, hyperdoped concentration, and crystallinity with etching time, from which we will discuss in detail why the photoresponse can be effectively improved by etching treatment.

In this experiment, we used a single-side-polished and boron-doped 300-μm-thick Si substrate wafer with a resistivity of 10 Ω cm cut to a size of 2×2 cm^2. After removing organic and metallic surface contaminants, the wafer was immediately placed on a translation stage in a vacuum chamber evacuated to less than 1×10^{-3} Pa. The chamber was filled with high-purity SF_6 gas at a pressure of 5×10^4 Pa. We irradiated the wafer using a 1 kHz, 100 fs, 800 nm Ti:sapphire laser with a snake-scanned route under various fluences. The laser was focused vertically on a 150-μm-diameter spot on the sample surface using a lens of 0.5 m focal length. Subsequently, a commercial 10-mm-diameter and 300-μm-thick Si-PIN photodiode was processed under the same conditions. After the fs laser processing, we intermittently etched the wafers and photodiodes with microstructures to study their optical and electrical properties by reactive ion etching (RIE) using SF_6 plasma under 50 W power and 30 mTorr pressure. The etching time interval was 20 s.

The morphologies of the surface microstructures were characterized by scanning electron microscopy (SEM). To analyze the absorption of microstructured Si, we measured the integrated reflectance (R) and transmittance (T) spectra between 1000 and 1200 nm in a PerkinElmer Lambda-1050 spectrometer equipped with a 160 mm integrating sphere, from which the integrated absorptance (A) spectra were extracted through $A = 1 - R - T$. The current versus bias properties and detector responsivity were characterized using a 1064 laser and Keithley 2450 source meter. In addition, the sulfur hyperdoping concentration distribution of the etched microstructure Si in the surface layer was measured by secondary ion mass spectrometry (SIMS) with a CAMECA 6F device using a 14.5 keV Cs+ primary beam at an incident angle of 25°. Finally, we used confocal Raman spectroscopy with a HeNe laser of 632 nm excitation wavelength to study

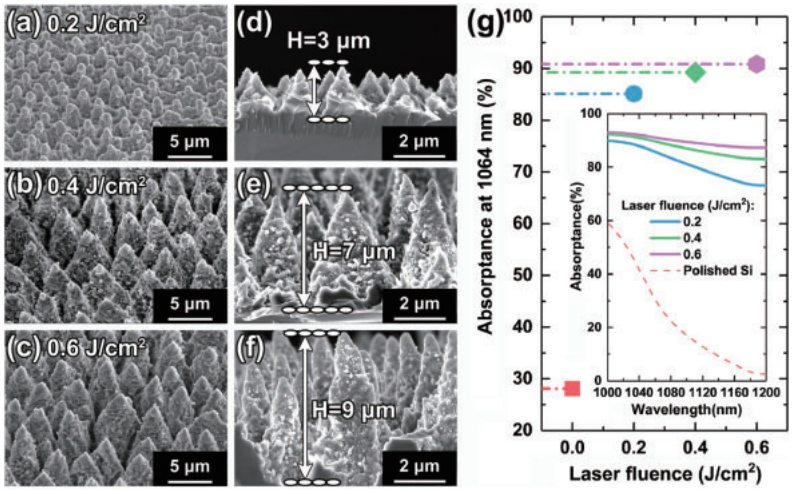

Fig. 1. SEM images of microstructured surface irradiated by fs laser at different fluences from two views: (a–c) tilt view (45°) and (d–f) side view. (g) 1064 nm absorption of microstructured Si at different fs laser fluences, with polished Si as a reference. Inset: absorption spectra of microstructured Si at different fs laser fluences.

the crystal properties in the surface layer of microstructured Si before and after the etching treatment.

To understand the influence of fs laser fluence on surface morphology, microstructured Si samples were fabricated by fs laser irradiation with different fluences. Figures 1(a)–1(f) show the evolution of surface morphology, where the laser fluences are 0.2, 0.4, and 0.6 J/cm^2. The surface morphology is composed of quasi-ordered microconical spike arrays and a large number of nanoparticles adhering to the spikes. Both the laser ablation and etching effects induced by dissociated SF_6 during fs laser processing lead to microstructure formation, which has been reported by several research groups.[2–6] As the laser fluence increases, the spike size also increases. The corresponding average spike heights that we obtained were 3, 7, and 9 μm. In particular, the increasing fluence roughened the spike surface seriously, and more nanoparticles were observed via enhanced laser ablation. Figure 1(g) shows the absorptance at 1064 nm as a function of laser fluence, where the inset presents the entire absorption spectra in the region from 1000 to 1200 nm. Owing to light falling on the edge of the Si band gap, the absorption coefficient at 1064 nm is as low as 10 cm^{-1}. Therefore, the 300-μm-thick polished Si layer without any laser irradiation had only a weak absorption of less than 30%. By contrast, after fs laser irradiation, the absorption markedly increased to 85% at the fluence of 0.2 J/cm^2. Further increasing the fluence led to a higher absorption. However, when it was 0.4 J/cm^2, the absorption tended to approach saturation. The absorption enhancement should be mainly attributed to the combination of large optical path length from large microstructures and sub-band-gap absorption of sulfur hyperdoping.[9,10] Additionally, the large number of nanoparticles and the high density of defects on a large microstructure surface also play a role in infrared light trapping.

Owing to near-infrared (NIR) absorption increase, it can be expected that the photoelectronic response should be considerably improved. To clarify this, we irradiated the back side of a commercial 10-mm-diameter and 300-μm-thick Si-PIN photodiode using a fs laser. Figure 2(a) shows the cross-sectional structure of the Si-PIN photodiode and the image of the diode back side after irradiation. The microstructure area that we prepared on the rear surface has a size of 4 × 4 mm^2. Figures 2(b) and 2(c) show the light current versus bias voltage and the extracted photoresponse at 1064 nm as a function of laser fluence, in which the results without laser irradiation are also given as a reference. At a low fluence, laser irradiation effectively improved the response of the Si diode owing to absorption enhancement, and it exhibited a linear dependence on laser fluence. The maximum response increased to 0.38 A/W at a laser fluence of 0.2 J/cm^2. However, with further fluence increase, the response began to decline dramatically. More seriously, the diode response was lower than that without laser irradiation when the laser fluence was beyond 0.4 J/cm^2, although it had a strong absorption. The response degradation at a high laser fluence should be attributed to several factors. First, subsurface phase transformations pressure-driven and induced by fs laser irradiation appear in Si, such as a-Si presenting a large number of structure defects and a high density of recombination sites. This can lead to a reduction in carrier lifetime.[21] Second, as the microstructure size increases, the carrier transport length will be less than the increasing thickness of the hyperdoped layer, which is a heavily disordered layer that contains a combination of nanocrystalline, microcrystalline, and amorphous regions overlaid on the fs-laser-induced spikes. Third, increasing the laser fluence will increase the hyperdoped sulfur concentration on the microstructured surface,[6] leading to a decrease in carrier mobility.[11] As a result, the combination of low carrier lifetime and mobility with high surface recombination velocities in surface microstructures extremely restricted the photoresponse improvement, although a high absorption can be obtained at a high laser fluence. Thus, to achieve a high NIR photoresponse, it is very necessary to control the disordered layer and hyperdoped concentration to promote the crystallinity of surface microstructures while maintaining a high NIR absorption.

To address these issues, we attempted a reactive ion etching (RIE) treatment to gradually peel off the top disordered layer overlying the microstructured Si irradiated with an intermediate fluence of 0.4 J/cm^2. As shown in Figs. 3(a)–3(f), the samples after 100, 200, and 300 s etchings were taken by SEM from different views, from which the surface morphology

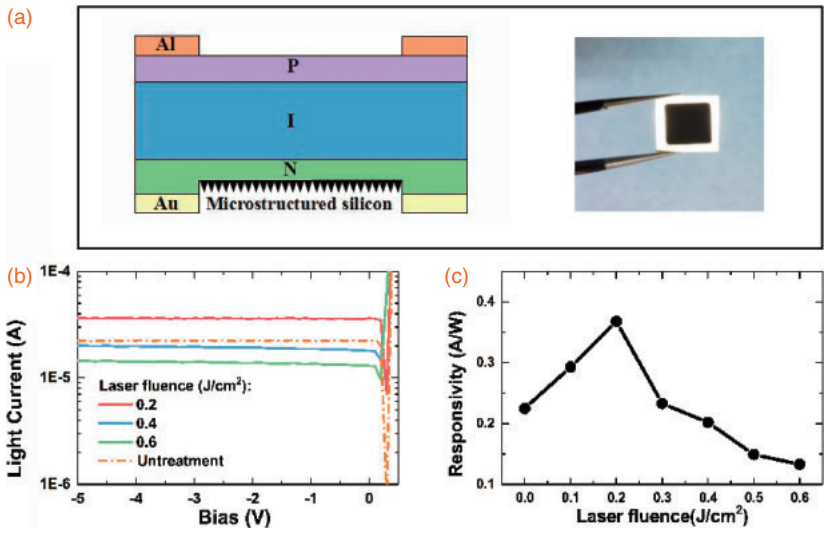

Fig. 2. (a) Cross-sectional structure of Si-PIN photodiode based on microstructured Si and real image of irradiated Si-PIN photodiode surface. (b) Light current versus bias voltage at 1064 nm as a function of laser fluence, with untreated photodiode as a reference and (c) extracted photoresponse at −5 V bias.

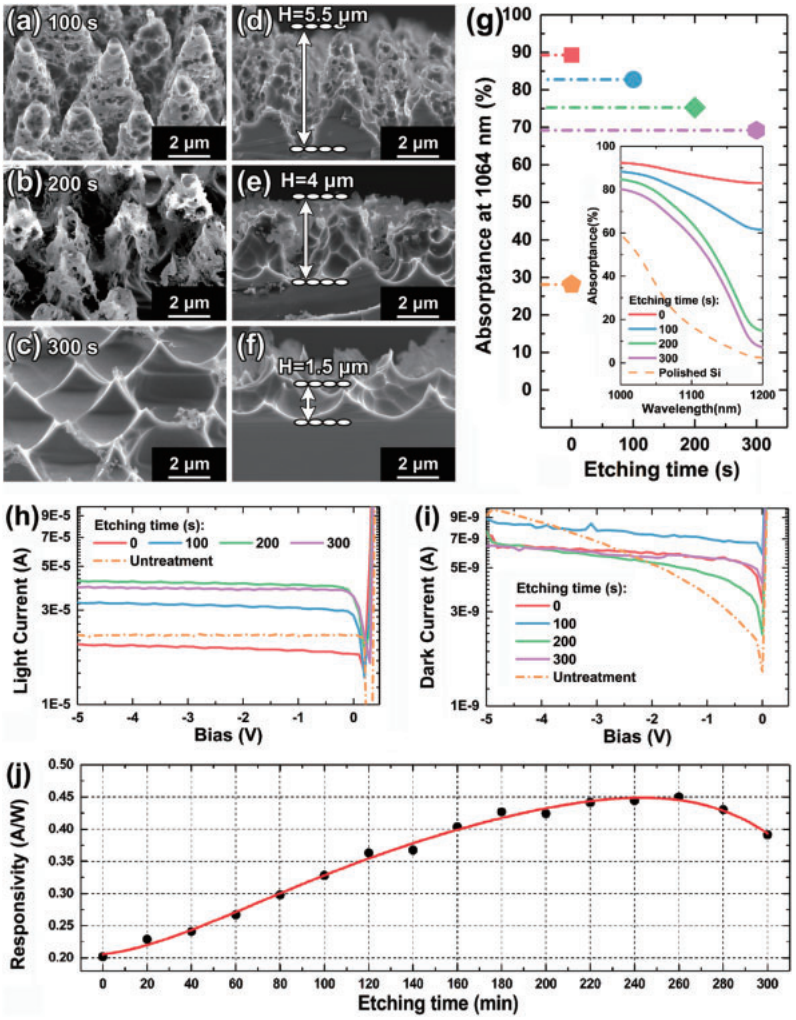

Fig. 3. SEM images of microstructured surface etched by RIE at different durations from two views: (a–c) tilt view (45°) and (d–f) side view. (g) 1064 nm absorption of microstructured Si at different etching times, with polished Si as a reference. Inset: absorption spectra of microstructured Si at different etching times. (h) Light current versus bias voltage and (i) dark current versus bias voltage of microstructured photodetectors at 1064 nm at different etching times, with untreated photodiode as a reference. (j) Extracted photoresponse at −5 V bias.

evolution can be observed well. At the initial stage of RIE treatment, a large number of nanoparticles and nanostructures adhering to the spikes disappeared, and the spike surface began to become smooth. As etching proceeded, the disordered layer with micrometer-scale structures was gradually cut down. Although the average height decreased to less than

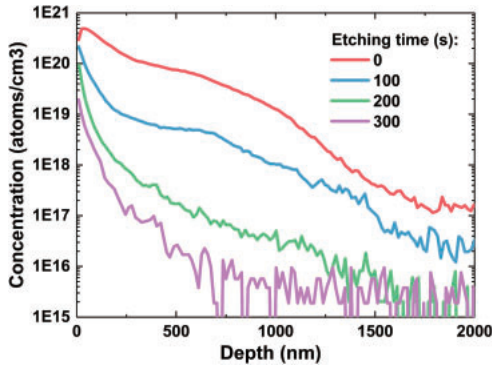

Fig. 4. Concentration profile of top sulfur hyperdoping layer etched at different durations.

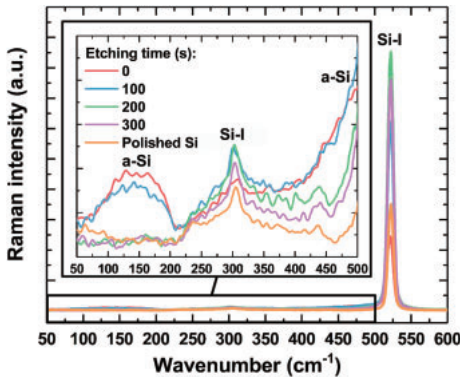

Fig. 5. Raman spectra of hyperdoped microstructured Si (fabricated with a fs laser pulse fluence of 0.4 J/cm^2) etched at different durations. Inset: Raman modes corresponding to a-Si and conventional crystalline silicon (Si-I), with polished Si as a reference.

2 μm, it still kept a conical spike profile after 300 s etching. Figure 3(g) shows the absorption at 1064 nm as a function of etching time, and the inset shows the absorption spectra from 1000 to 1200 nm. Owing to the spike size decrease, the absorption exhibited a degradation behavior. However, the absorption degradation with etching time at the short wavelength was completely different from that at the long wavelength. After 300 s etching, the absorption still had a high value of 70% at 1064 nm; however, it markedly decreased to a value less than 10% at 1200 nm. The serious absorption degradation at the long wavelength should be mainly attributed to the decrease in both hyperdoped thickness and concentration induced by RIE treatment. Figure 4 shows the sulfur dopant concentration profiles as a function of etching time. For the sample without any etching treatment, the fs-laser-induced sulfur dopant concentration at the uppermost 1 μm depth was more than 10^{19} cm^{-3}, which is several orders of magnitude greater than its solid solubility limit of 3×10^{16} cm^{-3} in Si crystals. In the case of hyperdoping, the electron–electron interaction couples the energy levels into an impurity or intermediate band near the bottom of the Si conduction band,[9,10] resulting in a high absorption close to 90% at around 1200 nm through sub-band-gap absorption. With etching time, the change in the hyperdoped concentration profiles shown in Fig. 4 clearly implies that the top hyperdoped layer is gradually removed by RIE treatment. This is why serious absorption degradation at around 1200 nm occurs.

Then, we continued to perform the RIE treatment on the microstructured area of the Si PIN diode irradiated by a 0.4 J/cm^2 fs laser. Figures 3(h) and 3(j) show the light current versus bias voltage and the extracted photoresponse at 1064 nm as a function of etching time, respectively, where the time interval is 20 s. As the etching progressed, the diode photoresponse showed a continuous increase before 200 s etching, reaching a peak of 0.45 A/W at around 250 s etching, which is clearly higher than the photoresponse (0.38 A/W) of the microstructured detector prepared at a low laser fluence of 0.2 J/cm^2, and begins to decrease after that. Moreover, the device dark current in Fig. 3(i) did not change significantly during etching and was still less than 10 nA. Considering the changes in surface morphology in Figs. 3(a)–3(f), we speculate that the photoresponse increase at 1064 nm induced by RIE treatment mainly originated from two factors. First, over time, continuous etching treatment peels off the conical microstructure gradually. As very clearly shown in Fig. 4, the etching treatment made the hyperdoped layer thinner and simultaneously reduced the sulfur hyperdoping concentration considerably by an order of magnitude. It was very conducive to carrier transport and carrier mobility increase.[11,12] Second, RIE treatment smooths the spike surface, removes the disordered layer, and decreases the number of surface structure defects acting as high-density recombination sites.[13–17] In other words, it repaired the crystallinity of the surface microstructures irradiated by the fs laser. This can be observed from the Raman measurements shown in Fig. 5. To begin with, the Raman spectra of the sample without RIE treatment exhibit several peaks (broad peaks at around 150 and 460–490 cm^{-1}) of a-Si produced by fs-laser-induced subsurface phase transformations.[18–20] However, it is interesting to note in Fig. 5 that, as the microstructure was sequentially peeled off, the Raman peaks of a-Si at around 150 and 460–490 cm^{-1} became weak and mostly disappeared after etching for 200 s. Moreover, the intensities of a-Si peaks decreased, while that of the crystal Si Raman peak at 522 cm^{-1} considerably increased as the etching treatment progressed. These experimental results indicate that the amount of a-Si generated during fs laser irradiation gradually decreases and that the crystallinity of spike microstructures improves after RIE treatment. This is very beneficial for the suppression of surface recombination and the promotion of carrier transport. As a result, RIE treatment can further enhance effectively the photoresponse of the Si PIN diode irradiated by a fs laser.

In conclusion, we have successfully demonstrated the photoresponse enhancement of fs-laser-irradiated Si photodiodes working at 1064 nm by intermittent RIE. We found that a short period of etching treatment can peel off the hyperdoped layer by an appropriate amount, control the dopant concentration, and repair the crystallinity and subsurface damage of hyperdoped microstructured Si induced by fs laser irradiation. We achieved a high photoresponse up to 0.45 A/W at 1064 nm in fs-laser-irradiated Si photodiodes by etching treatment. This processing method is very valuable for the manufacture of NIR-enhanced Si photodiodes.

Acknowledgment This work was supported by the National Natural Science Foundation of China (Grant Nos. 61675199 and U1435210).

1) M. A. Green and M. J. Keevers, Prog. Photovoltaics **3**, 189 (1995).
2) M. A. Sheehy, B. R. Tull, C. M. Friend, and E. Mazur, Mater. Sci. Eng. B **137**, 289 (2007).
3) T.-H. Her, R. J. Finlay, C. Wu, S. Deliwala, and E. Mazur, Appl. Phys. Lett.

73, 1673 (1998).
4) R. Younkin, E. Mazur, J. E. Carey, C. Crouch, J. A. Levinson, and C. M. Friend, J. Appl. Phys. **93**, 2626 (2003).
5) M. A. Sheehy, L. Winston, J. E. Carey, C. M. Friend, and E. Mazur, Chem. Mater. **17**, 3582 (2005).
6) C. H. Crouch, J. E. Carey, M. Shen, E. Mazur, and F. Y. Génin, Appl. Phys. A **79**, 1635 (2004).
7) J. Bonse, J. Krüger, S. Höhm, and A. Rosenfeld, J. Laser Appl. **24**, 042006 (2012).
8) E. L. Gurevich, Appl. Surf. Sci. **374**, 56 (2016).
9) H. Shao, C. Liang, Z. Zhu, B.-Y. Ning, X. Dong, X.-J. Ning, L. Zhao, and J. Zhuang, Appl. Phys. Express **6**, 085801 (2013).
10) H. Shao, Y. Li, J. Zhang, B.-Y. Ning, W. Zhang, X.-J. Ning, L. Zhao, and J. Zhuang, Europhys. Lett. **99**, 46005 (2012).
11) T. Zhang, B. Liu, W. Ahmad, Y. Xuan, X. Ying, Z. Liu, Z. Chen, and S. Li, Nanoscale Res. Lett. **12**, 522 (2017).
12) P. D. Persans, N. E. Berry, D. Recht, D. Hutchinson, H. Peterson, J. Clark, S. Charnvanichborikarn, J. S. Williams, A. DiFranzo, M. J. Aziz, and J. M. Warrender, Appl. Phys. Lett. **101**, 111105 (2012).
13) H. Sun, J. Xiao, S. Zhu, Y. Hu, G. Feng, J. Zhuang, and L. Zhao, Materials **10**, 351 (2017).
14) Y. Izawa, Y. Izawa, Y. Setsuhara, M. Hashida, M. Fujita, R. Sasaki, H. Nagai, and M. Yoshida, Appl. Phys. Lett. **90**, 044107 (2007).
15) J. Jia, M. Li, and C. V. Thompson, Appl. Phys. Lett. **84**, 3205 (2004).
16) X. Dong, N. Li, C. Liang, H. Sun, G. Feng, Z. Zhu, H. Shao, X. Rong, L. Zhao, and J. Zhuang, Appl. Phys. Express **6**, 081301 (2013).
17) M. Schade, O. Varlamova, J. Reif, H. Blumtritt, W. Erfurth, and H. S. Leipner, Anal. Bioanal. Chem. **396**, 1905 (2010).
18) M. J. Smith, Y. T. Lin, M. J. Sher, M. T. Winkler, E. Mazur, and S. Gradečak, J. Appl. Phys. **110**, 053524 (2011).
19) M. J. Smith, M. J. Sher, B. Franta, Y. T. Lin, E. Mazur, and S. Gradečak, J. Appl. Phys. **112**, 083518 (2012).
20) F. Costache, S. Kouteva-Arguirova, and J. Reif, Appl. Phys. A **79**, 1429 (2004).
21) M. Otto, M. Kroll, T. Kasebier, R. Salzer, A. Tunnermann, and R. B. Wehrspohn, Appl. Phys. Lett. **100**, 191603 (2012).